Applied Materials Today 19 (2020) 100587

Contents lists available at ScienceDirect

Applied Materials Today

journal homepage: www.elsevier.com/locate/apmt

Towards high-performance electrochemical thermal energy harvester based on ferrofluids

Marianna Vasilakaki [a], Ioulia Chikina [b], Valeri B. Shikin [c], Nikolaos Ntallis [a], Davide Peddis [d,e], Andrey A. Varlamov [f], Kalliopi N. Trohidou [a,*]

[a] Institute of Nanoscience and Nanotechnology, NCSR "Demokritos," Aghia Paraskevi, Attiki, 153 10, Greece
[b] IRAMIS, LIONS, UMR NIMBE 3299 CEA-CNRS, CEA-Saclay, F-91191 Gif-sur-Yvette Cedex, France
[c] Institute of Solid State Physics RAS, Chernogolovka, Moscow District 142432, Russia
[d] Dipartimento di Chimica e Chimica Industriale, Università di Genova, Via Dodecaneso 31, I-16146 Genova, Italy
[e] Istituto di Struttura della Materia-CNR, 00015 Monterotondo Scalo (RM), Italy
[f] CNR-SPIN, Viale del Politecnico 1, I-00133 Rome, Italy

ARTICLE INFO

Article history:
Received 18 July 2019
Received in revised form 23 January 2020
Accepted 25 January 2020

Keywords:
Seebeck coefficient
Thermoelectric nanomaterials
Magnetic nanoparticles

ABSTRACT

The ionic liquid-based thermo-electrochemical cells receive increasing attention as an inexpensive alternative to solid-state thermo-electrics for waste heat harvesting applications. Recently, it has been demonstrated that magnetic nanoparticles (MNPs) in liquid-based thermoelectric materials result in enhancement of the Seebeck effect opening new perspectives to the design of a thermoelectric device with relatively high efficiency and cost effectiveness. Here, the role of an interacting assembly of MNPs in the thermoelectric signal is studied for the first time. Based on a thermodynamic approach, an analytic expression has been derived for the Seebeck coefficient that includes the inter-particle magnetic interactions in the assembly and the nanoparticle's magnetic characteristics (saturation magnetization, magnetic anisotropy). Mesoscopic scale modelling with the implementation of the Monte Carlo Metropolis algorithm is performed to calculate their contribution to the Seebeck coefficient, for diluted assemblies of γ-Fe_2O_3 and $CoFe_2O_4$ nanoparticles, materials commonly used in ferrofluids. The results demonstrate the increase of the size and temperature range of the Seebeck coefficient with the increase of nanoparticles' magnetic anisotropy paving the way for the detailed study of the magneto-thermal effects in high-performance thermoelectric materials based on ferrofluids.

1. Introduction

The urgent need for an increased energy production from renewable resources has rapidly advanced the research towards inexpensive and low-toxicity thermoelectric materials for the design of thermal energy harvesting devices, that they will not produce emissions and will not consume materials. The ionic liquid-based thermo-electrochemical cells [1–3] are promising candidates that meet these requirements. As in the case of the solid state based thermoelectric materials, when a thermal gradient is applied in a liquid-based thermoelectric material, the mobile charge carriers (the ions) diffuse towards the cold side, where this accumulation of charge creates a potential difference. This is the well-known Seebeck effect [1] and the voltage generated per unit temperature is the Seebeck coefficient. In the case of thermocells based on a redox-active electrolyte, the Seebeck coefficient can be of the order of mV K^{-1} [1]. So these thermocells can be interesting alternatives to the solid-state devices for thermal energy harvesting.

The efforts to enhance the Seebeck coefficient have mainly been focused on the improvement of the liquid [4,5], the redox couples [6], the electrodes [3] or by introducing thermoplastic fluoro-polymeric membranes [2].

Recently a breakthrough to the enhancement of the thermoelectric efficiency of ionic liquid-based thermo-electrochemical cells has been achieved by introducing in the ionic liquids dispersions of magnetic nanoparticles [7,8]. The thermodiffusion behavior of these charged colloidal suspensions with contributions from both electrolytes and the charged colloidal particles influences the Seebeck effect [7]. Indeed, recent experimental studies have demonstrated that the Seebeck coefficient of liquid thermoelectric

* Corresponding author.
E-mail address: k.trohidou@inn.demokritos.gr (K.N. Trohidou).

https://doi.org/10.1016/j.apmt.2020.100587

materials can be increased by 15% [7–9], by using MNPs dispersed in liquid electrolytes with volume fraction ~1%.

The presence of nano-entities plays a crucial role in the thermoelectric performance of liquid-based thermoelectric materials, as in the case of nanostructured bulk [10] or nanoparticle based (system of Co nanoparticles (5–10 nm) dispersed in $Ba_{0.3}In_{0.3}Co_4Sb_{12}$ matrix [11]) solid state thermoelectric materials. These nano-entities make the physical profile of the studied system very complicated and consequently it is rather difficult to understand its properties. Therefore, the contribution of theoretical calculations and predictions in the development of advanced high-performance thermoelectrics, that has already been demonstrated to be very important for solid-state nanostructured thermoelectric materials [10,12], becomes very significant for this new class of materials, that combine ionic liquids and magnetic nanoparticles, i.e. the ionic liquid based ferrofluids.

In this context, we study for the first time the role of a magnetic nanoparticle assembly in the enhancement of the thermoelectric signal. Initially, an analytic expression is derived for the chemical potential and its temperature derivative taking into account the inter-particle magnetic interactions in the assembly and the nanoparticle's magnetic anisotropy. The Monte Carlo (MC) simulations technique with the implementation of the Metropolis Algorithm [13] is used to calculate the system's temperature depended energy and the temperature derivative of the chemical potential ($d\mu/dT$). The temperature dependence of the Seebeck coefficient is calculated from the Kelvin formula [14,15] that relates the Seebeck coefficient to the temperature derivative of the chemical potential μ of the system.

Our study is focused on the effect of the magnetic contributions to the Seebeck coefficient of a dilute system of MNPs with special attention on the effect of nanoparticle's magnetic anisotropy [16].

Interestingly, our MC simulations demonstrate that the increase in the magnetic anisotropy blocks temporarily the thermally induced switching of the magnetization vector in each nanoparticle for a wide temperature range, resulting to the enhancement of the overall response of the chemical potential variation to the applied thermal gradient and consequently to the Seebeck coefficient. A finding which is very important for the use of magnetic nanoparticle based materials in electro/magnetothermal applications.

2. The Model and the calculation of the Seebeck coefficient

The total Seebeck coefficient S_{tot} of the system that consists of all the subsystems of the carriers (ions of electrolytes, interacting magnetic nanoparticles, electrodes), the thermoelectric coefficient β_{tot} and the electrical conductivity σ_{tot} are related as [17] (see Supporting Information SI1 for details):

$$S_{tot} = -\beta_{tot}/\sigma_{tot} \tag{1}$$

In the case of a broken external circuit (no current, the voltmeter of infinite resistance), the S_{tot} is related to the temperature derivative of the chemical potential μ_ℓ by the Kelvin formula [14] for constant carrier number N_ℓ and charge Q_ℓ of each non-interacting subsystem as :

$$S_{tot} = \sum_\ell \frac{1}{Q_\ell}\left(\frac{d\mu_\ell}{dT}\right)_{N_\ell} \tag{2}$$

We must note that we use the full derivative since we consider fixed number N_ℓ [18].

The conductivity can be expressed as a function of the mobility η_ℓ, the charge Q_ℓ and the number of carriers N_ℓ of the ℓth non-interacting subsystem as $\sigma_\ell = \eta_\ell N_\ell Q_\ell$. Thus, combining Eqs. (1) and (2) the thermoelectric conductivity reads:

$$\beta_{tot} = \sum_\ell \beta_\ell = -\sum_\ell S_\ell \sigma_\ell = -\sum_\ell \eta_\ell N_\ell \left(\frac{d\mu_\ell}{dT}\right)_{N_\ell} \tag{3}$$

Using Eq. (3), we can rewrite Eq. (1) for the total Seebeck coefficient as:

$$S_{tot} = \frac{\sum_\ell \eta_\ell N_\ell \left(\frac{d\mu_\ell}{dT}\right)_{N_\ell}}{\sum_\ell \eta_\ell N_\ell Q_\ell} \tag{4}$$

As we have stated above, here we focus on the new term in S_{tot}, namely the contribution to the Seebeck coefficient S_{np} coming from the subsystem of interacting magnetic nanoparticles ($\ell = np$) added in the ionic liquid. This term for a given total conductivity and number of magnetic nanoparticles N_{np} is given by the expression:

$$S_{np} = -\frac{\beta_{np}}{\sigma_{tot}} = \frac{\eta_{np} N_{np}\left(\frac{d\mu_i}{dT}\right)_{N_{np}}}{\sum_\ell \eta_\ell N_\ell Q_\ell} \tag{5}$$

The chemical potential μ_i is defined as the energy which is in average necessary to be paid in order the ith particle to be added in the thermodynamic system. The statistical average of the this energy over the M microstates of a canonical ensemble is given by the expression [13]:

$$\mu_i = < E_i > = \frac{\sum_q^M E_{i,q} \exp(-\frac{E_{i,q}}{T})}{\sum_p^M exp(-\frac{E_{i,p}}{T})} \tag{6}$$

where the brackets denote the thermal average. In our study this energy is calculated with the implementation of the Metropolis Monte Carlo algorithm.

Combining Eqs. (5) and (6) for a given total conductivity and particles' mobility, we calculate the temperature derivative of the chemical potential and from this we find the Seebeck coefficient of the nanoparticle assembly:

$$S_{np}(T, N_{np}) = \frac{\eta_{np} N_{np}}{\sigma_{tot}}\left(\frac{d\mu_i}{dT}\right)_{N_{np}} = \frac{\eta_{np} N_{np}}{\sigma_{tot}}\left(\frac{d < E_i >}{dT}\right)$$
$$= \frac{\eta_{np}}{\sigma_{tot}}\left(\frac{d < E >}{dT}\right) \tag{7}$$

In our model for the description of a nanoparticle, we use the single-spin approach, the Stoner-Wohlfarth model of the coherent rotation of a particle's magnetization [19]. We employ this model considering an effective spin described by a three-dimensional classical vector, ${}^s i$ $i = 1,..,N_{np}$ (N_{np} the total number of particles), to represent the magnetic moment of each nanoparticle of volume V and saturation magnetization M_S. Each nanoparticle possesses uniaxial magnetic anisotropy with an easy anisotropy axis oriented in a random direction [20]. To derive <E>, we consider the system of N_{np} identical spherical magnetic nanoparticles of diameter (d), located randomly at the nodes of a simple cubic lattice inside a box of $15a \times 15a \times 15a$ where a is the lattice constant.

The total energy of the system of the N_{np} nanoparticles is:

$$E = E_{dip} + E_k = g_{np} \sum_{i>j}^{N_{np}} \frac{(\hat{s}_i \cdot \hat{s}_j) - 3(\hat{s}_i \cdot \hat{r}_{ij}) \cdot (\hat{s}_j \cdot \hat{r}_{ij})}{\hat{r}_{ij}^3}$$
$$- \sum_{i=1}^{N_{np}} K_{eff} V \left(\hat{s}_i \cdot \hat{e}_i\right)^2 \tag{8}$$

The first term gives the dipolar interactions among all spins in the nanoparticle assembly with dipolar strength g_{np} =

$\mu_0(M_S V)^2/(4\pi\, d^3)$, where d is the nanoparticle size, since it is the smallest distance between two spherical nanoparticles. The second energy term gives the anisotropy energy with anisotropy strength K_{eff} of a particle with volume V. This is an effective anisotropy that includes the nanoparticle's surface anisotropy, the magneto-crystalline anisotropy, the strain and shape anisotropy. Here $\hat{e}_i$ is the anisotropy axis random direction for the ith nanoparticle. The thermal energy is $k_B T$ (where T is the temperature and k_B the Boltzmann constant).

The energy parameters g_{np} and K_{eff}, as they are entered into the simulations, are normalized to the thermal energy $k_B T$ at T = 5 K, so they are dimensionless. The reduced dipolar strength is denoted by g and the reduced magnetic anisotropy by k. The effective anisotropy is assumed uniaxial [16]. For the dipolar energy calculation free boundary conditions in all directions have been taken into account, since a frozen ferrofluid is simulated.

For each temperature T_i, the thermal average of the magnetic energy $<E(T_i)>$ is calculated.

The equilibrium configurations of the system are obtained from the minimization of the total energy using the Monte Carlo technique and the Metropolis algorithm [13]. For each temperature, the first 500 steps per spin are used for equilibration, and the subsequent 5000MC steps are used to obtain thermal averages from simple arithmetic averages over the accepted configurations. The Monte Carlo simulations results of the total energy for a given temperature were averaged over 60 samples with various spin configurations, realizations of the easy-axes distribution and different spatial configurations for the nanoparticles.

Next, the temperature derivative of the thermal average of the magnetic energy which is proportional to the particle Seebeck coefficient S_{np} (see Eq. (7)) is calculated. It is defined as the average of the slopes between the energy at the temperature intervals $[T_{i-1}, T_i]$ and $[T_i, T_{i+1}]$ respectively, $\frac{d<E(T_i)>}{dT} = \frac{1}{2}\left(\frac{<E(T_{i+1})>-<E(T_i)>}{T_{i+1}-T_i} + \frac{<E(T_i)>-<E(T_{i-1})>}{T_i-T_{i-1}}\right)$ where $T_{i-1}=T_i-\Delta T$ and $T_{i+1} = T_i + \Delta T$ with ΔT being a constant temperature step. We consider ΔT = 10 K, as it is commonly used in the experiments [7].

Finally, we divide the Seebeck coefficient (Eq. (7)) with the quantity $(\eta_{np}\ k_B)/\sigma_{tot}$, where σ_{tot} is the electrical conductivity of the system and η_{np} the nanoparticles mobility, and we calculate in this way the reduced particle Seebeck coefficient S_{np} at average temperature T, which is dimensionless.

The statistical error is negligible, so it does not appear in our plots.

3. Results and discussion

We examine the effect of the anisotropy strength of the magnetic nanoparticles to the formation of the thermo-power signal. We consider two types of magnetic nanoparticle systems, commonly used in biomedical, energy and industrial ferrofluid applications [7,21–23]: one consisting of maghemite and the second of Co ferrite nanoparticles with varying anisotropy strengths.

In order to study the effect of the magnetostatic inter-particle interactions in the assemblies, we consider, in all cases of the nanoparticles assemblies, two different nanoparticle concentrations, a dilute one with c = 1.0% and a denser one (however well below the percolation threshold) with c = 4.7%.

Our aim is to study the factors that influence the experimentally observed behavior and to propose materials with the optimized magnetic properties for the magneto-thermal applications.

First we estimate the energy parameters entering in the Eq. (8), for maghemite nanoparticles. We start from the reported experimental values for their saturation magnetization and their effective anisotropy. In the literature different effective magnetic anisotropy strengths have been reported for the same type and similar size of the maghemite nanoparticles that have been attributed to different structures resulting from different methods of production or different deposition conditions. We consider four cases: (a) spherical maghemite nanoparticles of mean diameter 7 nm dispersed in a polymer matrix [24] with $K_{eff} = 6{\cdot}10^3$ J m^{-3} (k = 33.7 at T = 5 K), (b) colloidal maghemite nanoparticles of similar mean size with case (a) (the anisotropy strength reported in this case is $1.2{\cdot}10^4$ J m^{-3} [25] (k = 67.4 at T = 5 K)), (c) maghemite nanoparticles coated with silica shell of 12.5 nm size having much larger anisotropy $3{\cdot}10^4$ J m^{-3} (k = 168.5 at T = 5 K) [26] and (d) 9 nm maghemite nanoparticles produced by a physical method, the laser target evaporation technique having the largest effective anisotropy of $1.2{\cdot}10^5$ J m^{-3} (k = 673.8 at T = 5 K)) [27]. These differences in the anisotropy have been also observed in other systems and depend on size and surface effects [27,28], on strain effects and on the presence of structural defects [29].

For the studied maghemite nanoparticles, we consider saturation magnetization M_S = 249 kA m^{-1} at 5 K, M_S = 215 kA m^{-1} at 300 K and size d = 9 nm, which are typical values for nanoparticles in ionic liquid based ferrofluids [30]. This saturation magnetization M_S decreases from its T = 5 K value following a power law T^{α} with a = 2.3, that affects the magnetization processes in nanoparticle systems in agreement with experimental findings [27]:

$$M_S(\mathrm{T}) = M_S(5\mathrm{K}) - b{\cdot}T^{2.3} \tag{9}$$

where $b = 6.8{\cdot}10^{-2}$ Am^{-1} K$^{-2.3}$. This temperature dependence is extracted from the Bloch law as modified taking into account the finite size effects in the nanoparticles [31].

Since the dipolar strength is proportional to $M_S{}^2\,(T)$, we have $g(T) = c_1{\cdot}M_S{}^2(T) = c_1{\cdot}(M_S\ (5\ \mathrm{K}) - b{\cdot}T^{2.3})^2 = c_1{\cdot}(M_S{}^2\ (5\ \mathrm{K}) - 2\ M_S\ (5\ \mathrm{K}){\cdot}b{\cdot}T^{2.3} + b^2{\cdot}T^{4.6})$ with $c_1 = \mu_0 V^2/(4\pi d^3{\cdot}k_B T(5\ K)) = 2.75{\cdot}10^{-10}$ A$^{-2}{\cdot}$m^2 and M_S (5 K) = 249 kA m^{-1} [27], then $g(5\ \mathrm{K}) = c_1{\cdot}M_S{}^2(5\ K) = 17$. So at a first approximation, keeping the first two terms, we get

$$g(T) = 17 - b_1{\cdot}T^{2.3} \tag{10}$$

where $b_1 = 2{\cdot}c_1{\cdot}M_S\ (5\ \mathrm{K}){\cdot}b = 9{\cdot}10^{-6}$ A m^{-1} K$^{-2.3}$.

Therefore $g(T)$ follows the power law temperature dependence of M_S.

In the literature, the temperature dependence of the effective anisotropy strength appears to be different for the different types of anisotropy (cubic, uniaxial) and the internal structure of the nanoparticles (interaction between the sublattices, surface) [32,33]. It is demonstrated that for ferrite nanoparticles with uniaxial anisotropy (as in our case), $k(T) \sim M_S\ (T)^2$ [33], as for $g(T)$ therefore $k(T) \sim T^{2.3}$ at a first approximation, or $k(T) \sim M_S\ (T)$ [34]. Taking into account the above considerations, we assume that $k(T)$ follows the same temperature dependence as M_s. We consider a reduced temperature dependent anisotropy:

$$k(T) = k(T = 5\mathrm{K}) - b_2{\cdot}T^{2.3} \tag{11}$$

where b_2 is such that $k(300\ \mathrm{K})/k(5\ \mathrm{K}) = 85\%$ as in the $M_S\ (300\ \mathrm{K})/M_S\ (5\ \mathrm{K})$ case. So in our simulations the effective anisotropy strengths for the maghemite nanoparticles that we consider, at T = 5 K, are: k (T = 5 K) = 33.7, 67.4, 168.5, 673.8, the corresponding b_2 values, in Eq. (11), are shown in Table 1.

Initially, we calculate the Seebeck coefficient S_{np} for 7 nm maghemite nanoparticles with low anisotropy (k = 33.7 at T = 5 K) from Reference [24] and we compare our results with the zero anisotropy maghemite nanoparticles (k = 0, see Supporting Information SI2) case, in order to study the effect of the dipolar interactions. Fig. 1 shows the dependence of the reduced Seebeck coefficient on the average temperature T for the two magnetic nanoparticle systems concentrations. Interestingly, by introducing a weak effective anisotropy, we observe in Fig. 1 that the $S_{np}(T)$

Table 1
The experimental values of the saturation magnetization M_s and the anisotropy K_{eff} (T = 5 K) strengths (three first columns), together with the calculated from Eq. (10) and (11) dipolar g and anisotropy k strengths as a function of the temperature T (last two columns) for the γ-Fe_2O_3.

	M_s(5 K) [kAm^{-1}]	M_s(300 K) [kAm^{-1}]	K_{eff}(5 K) [$\cdot 10^5$ J m^{-3}]	$g(T)$	$k(T)$
γ-Fe_2O_3 NPs					
	249	215	0.06	$17–9\cdot10^{-6}\cdot T^{2.3}$	$33.7–10^{-5}\cdot T^{2.3}$
			0.12	$17–9\cdot10^{-6}\cdot T^{2.3}$	$67.4–2\cdot10^{-5}\cdot T^{2.3}$
			0.3	$17–9\cdot10^{-6}\cdot T^{2.3}$	$168.5–5\cdot10^{-5}\cdot T^{2.3}$
			1.2	$17–9\cdot10^{-6}\cdot T^{2.3}$	$673.8–2\cdot10^{-4}\cdot T^{2.3}$

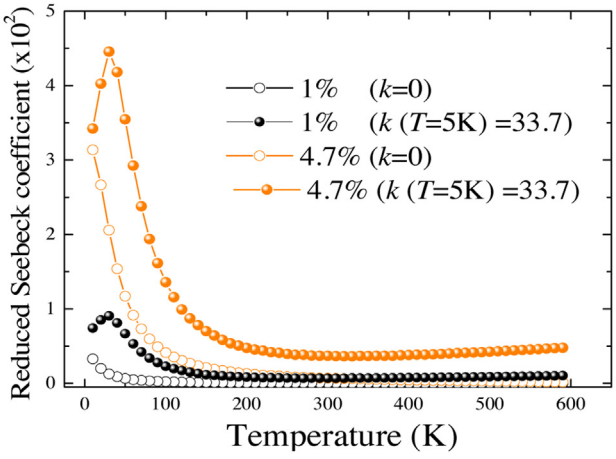

Fig. 1. Reduced Seebeck coefficient (S_{np}) as a function of average temperature T for concentration c = 1% (black) and c = 4.7% (orange) and effective magnetic particle anisotropy k = 0 (open symbols) and $k \neq 0$ (closed symbols). The dipolar and anisotropy strengths are temperature dependent with g = 17 and k = 33.7 at temperature T = 5 K.

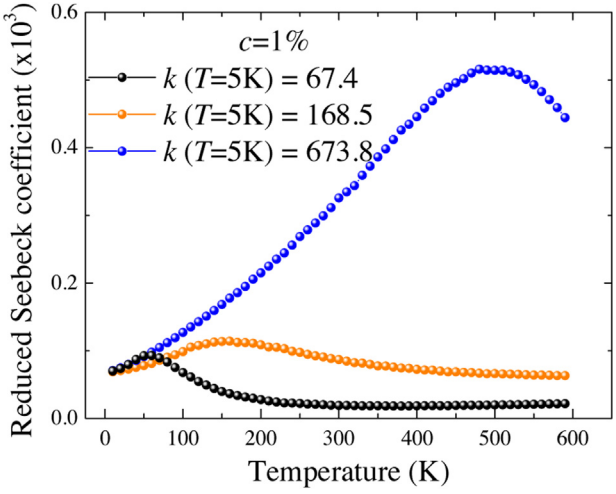

Fig. 2. Reduced Seebeck coefficient (S_{np}) as a function of average temperature T for an interacting assembly of maghemite particles (concentration c = 1%) with T-dependent g and k, for the three different anisotropy strengths: k = 67.4 (black), 168.5 (orange), 673.8(blue) at T = 5 K.

curve departs from the monotonic T dependence of the k = 0 case (see Fig. S1b,c, Supporting Information). Importantly, in the finite k case, the $S_{np}(T)$ curve shows a maximum for both concentrations c = 1% and 4.7% at T = 30 K. As it has been demonstrated in Supporting Information SI2, $S_{np}(T)$ increases with the increase of the particle concentration.

Next, we calculate the Seebeck coefficient for 1% particle concentration (Fig. 2) for higher anisotropies of maghemite nanoparticles [25–27]. We consider three different temperature dependent anisotropy strengths k (T = 5 K) = 67.4, 168.5 and 673.8. The temperature dependence of the dipolar strength is also taken into account (with $g(T$ = 5 K) = 17). Our MC simulations results in Fig. 2 show that the increase of the particle's anisotropy enhances the reduced S_{np}. We observe that the reduced Seebeck coefficient increases with the increase of the anisotropy for temperatures above T = 100 K. Also the maximum of the $S_{np}(T)$ curve shifts to higher average T with the increase of the effective anisotropy. Therefore, the Seebeck coefficient for enhanced magnetic anisotropies follows non-monotonic temperature dependence. The temperature at which the maximum occurs and its value depend on the anisotropy strength.

In our systems, as a magnetic particle enters into the magnetic assembly then a re-orientation of the magnetic moments occurs in order to reduce the magneto static interaction energy. This re-orientation of the particle's moment is affected by the interplay between its magnetic anisotropy and the interparticle interaction energy. For high anisotropy (hard) nanoparticles at low enough temperatures, the spins are almost frozen and as a result the energy difference before and after the insertion of the particle is big, consequently the Seebeck coefficient increases in comparison with that of the magnetically soft nanoparticles as it can be seen in Fig. 2. The anisotropy prevents the thermal switching of the spins, so they are almost blocked for a wide range of temperatures. This range of temperatures depends on the anisotropy strength of the nanoparticles. As the temperature increases, near the blocking temperature T_B of the system, that depends on the anisotropy strength [35], the thermal energy overcomes the anisotropy energy barrier, the spins become unblocked and the chemical potential drops rapidly with temperature, therefore it gives a high gradient, i.e. Seebeck coefficient. Near the T_B, the Seebeck coefficient reaches its maximum value and then it drops. As we can see in Fig. 2, the highest the blocking temperature, since it is proportional to the anisotropy strength, the highest the temperature at which the maximum of the $d\mu/dT$ occurs. In Fig. 2, we observe a widening of the temperature range where Seebeck coefficient has values around 90% of its maximum value as the anisotropy increases. For instance, ~2.5 times increase of the anisotropy strength (from k = 67.4 to k = 168.5), results in an almost 3 times widening of the $S_{np}(T)$ curve. However, this behavior is non-systematic, because of the different temperature dependence of the magnetization and the anisotropy, so for the maximum anisotropy strength (k = 673.8) the widening is ~1.3 times the one for the 4 times lower anisotropy (k = 168.3).

Finally, we study the Seebeck coefficient for $CoFe_2O_4$ nanoparticles, which they have much higher anisotropy than the maghemite ones and they are coated with two organic surfactants, attached to nanoparticles by a hydroxylic and a carboxylic group. This is the common practice in order to make them environmentally friendly, stable in solution and therefore suitable for applications. Our results are compared with the ones for uncoated $CoFe_2O_4$ nanoparticles.

First we estimate the energy parameters entering Eq. (8), for these nanoparticles. The oleic acid coated Co ferrite nanoparticles (d = 5 nm) have an effective anisotropy $7.4\cdot10^5$ J m^{-3} (k = 700 at T = 5 K) and the diethylene glycol coated nanoparticles have an effective anisotropy $4.8\cdot10^5$ J m^{-3} (k = 455 at T = 5 K), as it is reported in Reference [21]. The $CoFe_2O_4$ nanoparticles show higher effective anisotropy $8.8\cdot10^5$ J m^{-3} (k = 832 at T = 5 K) than the coated

Table 2
The experimental values of the saturation magnetization M_s and the anisotropy K_{eff} (T = 5 K) strengths (three first columns), together with the calculated from Eq. (10) and (11) dipolar g and anisotropy k strengths as a function of the temperature T (last two columns) for the Co Fe_2O_4 nanoparticles (uncoated and coated with Oleic acid or Diethylene glycol) [21,36,42].

	M_s(5 K) [kAm^{-1}]	M_s(300 K) [kAm^{-1}]	K_{eff}(5 K) [$\cdot 10^5$ J m^{-3}]	$g(T)$	$k(T)$
$CoFe_2O_3$ NPs					
Oleic acid	432	333	7.4	$9.3–8\cdot10^{-6}\cdot T^{2.3}$	$700–3\cdot10^{-4}\cdot T^{2.3}$
Diethylene glycol	624	572	4.8	$19.4–6\cdot10^{-6}\cdot T^{2.3}$	$455–7\cdot10^{-5}\cdot T^{2.3}$
Uncoated	381	305	8.8	$7.2–5\cdot10^{-6}\cdot T^{2.3}$	$832–3\cdot10^{-4}\cdot T^{2.3}$

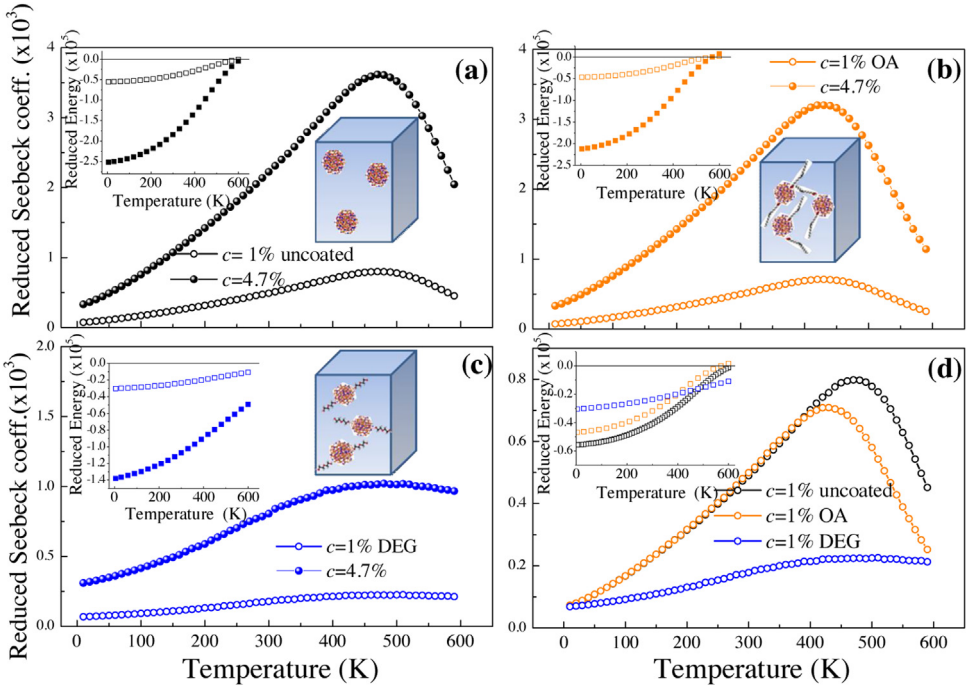

Fig. 3. Reduced Seebeck coefficient of $CoFe_2O_4$ nanoparticles as a function of the average temperature T for two concentrations c = 1% (open symbols) and c = 4.7% (closed symbols) for a) uncoated nanoparticles (black), b) oleic acid (OA) coated (orange), c) diethylene glycol (DEG) coated nanoparticles (blue) and d) comparison of the different coatings for c = 1%. Insets: The thermal average energy <E> that includes the dipolar energy and the anisotropy energy terms with temperature dependent g and k for the two particle concentrations.

ones, as it has been shown by our Density Functional Theory (DFT) calculations [36] and experimental findings [37].

For the Co ferrite nanoparticles [38–40], we consider the same temperature dependence of M_S, g and k with the maghemite nanoparticles (Eqs. (9), (10) and (11)). The saturation magnetization for the diethylene glycol coated samples is taken M_S = 624 kA m^{-1} at T = 5 K and for T = 300 K M_S = 572 kA m^{-1} [21], and for the oleic acid coated samples M_S(5 K) = 432 kA m^{-1} and M_S(300 K)=333 kA m^{-1}, as they are reported in Reference [21]. For the uncoated Co ferrite particles, we estimate M_S(5 K) = 381 kA m^{-1} based on our DFT calculations [36] and at 300 K we consider a 20% reduced M_S(300 K) = 305 kA m^{-1} based on Reference [41], b_1 and b_2 in the case of Co ferrite nanoparticles are shown in Table 2. The ratio k(300 K)/k(5 K) is the same with the ratio of M_s(300 K)/M_s(5 K). The values of the effective anisotropy strength used in our simulations are k(T = 5 K) = 455, 700, 832, derived from the corresponding experimental ones.

We calculate the total energy <E> and the $S_{np}(T)$ for the concentrations 1% and 4.7% (Fig. 3a,b,c respectively). For these nanoparticles the anisotropy term dominates over the dipolar energy term. Notably, in the case of diethylene glycol coated nanoparticles, the M_S and the effective magnetic anisotropy k decreases only 8% from T = 5 K to T = 300 K, contrary to the other two cases where the decrease is around 20% [21]. This results to a broader maximum of the $S_{np}(T)$ curve in the case of diethylene glycol coating comparing to the other cases, covering a broader temperature range 400–600 K (Fig. 3d). Consequently, our study demonstrates that it will be advantageous for thermoelectric applications to use MNPs with high magnetic anisotropy weakly temperature dependent, in order to obtain the maximum of the Seebeck coefficient for a broad temperature range, especially at temperatures above 300 K.

As we observed from Fig. 3, the overall behavior of the Co ferrite nanoparticles system is similar to that of the maghemite nanoparticles Figs. 1 and 2. However the relative sizes of the Seebeck coefficient of the Co ferrite nanoparticles is bigger than that of the maghemite nanoparticles in all cases because of the larger anisotropy.

Interestingly, the behavior of the reduced $S_{np}(T)$ curve for diethylene glycol coated $CoFe_2O_4$ nanoparticles is similar to the behavior of the measured Seebeck coefficient (T) curve for the recently reported novel nanoparticle based solid state thermoelectric system [11] which shows a large plateau at the temperature range of 700–850 K. This similarity illustrates the possibility of tuning the Seebeck coefficient in ferrofluid — based thermo-electrics by varying the nanoparticles concentration and the magnetic particle anisotropy and achieving enhanced thermoelectric properties comparable or even better than those of their solid state counterparts.

4. Conclusion

The role of the thermomagnetic contribution in the formation of an enhanced thermoelectric signal in diluted magnetic nanoparticle assemblies has been studied for the first time by calculating the Seebeck coefficient. An analytic expression for the Seebeck coefficient of the assembly of MNPs has been derived, taking into account the single particle anisotropy and their magnetostatic interparticle interactions. Our MC calculations performed on γ-Fe_2O_3 and $CoFe_2O_4$ dilute nanoparticles' assemblies show that the Seebeck coefficient of the system depends non-monotonously on temperature and its magnitude depends strongly on the particle concentration and the nanoparticle's anisotropy strength. The strong magnetic anisotropy enhances the Seebeck coefficient and as it increases, it shifts its maximum at higher temperatures. Interestingly, in the weak temperature dependent anisotropy case, the maximum of the Seebeck coefficient broadens. Thus optimum performance can be accomplished for a larger temperature range, as in the case of diethylene glycol coated $CoFe_2O_4$ nanoparticles. Our approach provides a new insight into the nanoscale phenomena that govern the properties of complex thermo-electro-magnetic materials. Apparently, the magnetic anisotropy induces thermal stability of the nanoparticles delaying their thermally activated magnetization reversal for a broad range of temperatures resulting also to an increase in the temperature derivative of the chemical potential at higher temperatures. The results illustrate the potential of the new research direction proposed in this study: magnetic nanoparticles with high magnetic anisotropy for ionic liquid-based thermo-electric devices in order to achieve enhanced Seebeck coefficients at higher temperatures.

Data availability

The raw/processed data required to reproduce these findings cannot be shared at this time as the data also forms part of an ongoing study.

Conflict of interest

The authors declare no conflict of interest.

CRediT authorship contribution statement

Marianna Vasilakaki: Methodology, Formal analysis, Software, Writing - review & editing, Visualization. **Ioulia Chikina:** Methodology, Formal analysis, Writing - review & editing. **Valeri B. Shikin:** Methodology, Formal analysis, Writing - review & editing. **Nikolaos Ntallis:** Methodology, Formal analysis, Software, Writing - review & editing. **Davide Peddis:** Writing - review & editing. **Andrey A. Varlamov:** Methodology, Formal analysis, Writing - review & editing. **Kalliopi N. Trohidou:** Methodology, Formal analysis, Software, Writing - review & editing, Visualization, Funding acquisition.

Acknowledgements

This work was supported by the European Union's Horizon 2020 Research and Innovation Programme: under grant agreement No. 731976 (MAGENTA). KNT, MV and NN acknowledge the computational time granted from the Greek Research & Technology Network (GRNET) in the Greek National HPC facility ARIS (http://hpc.grnet.gr) under project MNBIE (pr005030).

Appendix A. Supplementary data

Supplementary material related to this article can be found, in the online version, at https://doi.org/10.1016/j.apmt.2020.100587.

References

[1] M.F. Dupont, D.R. MacFarlane, J.M. Pringle, Thermo-electrochemical cells for waste heat harvesting – progress and perspectives, Chem. Commun. (Camb.) 53 (2017) 6288–6302, http://dx.doi.org/10.1039/C7CC02160G.
[2] S.W. Hasan, S.M. Said, M.F.M. Sabri, A.S.A. Bakar, N.A. Hashim, M.M.I.M. Hasnan, J.M. Pringle, D.R. MacFarlane, High thermal gradient in thermo-electrochemical cells by insertion of a poly(Vinylidene fluoride) membrane, Sci. Rep. 6 (2016) 1–11, http://dx.doi.org/10.1038/srep29328.
[3] H. Im, T. Kim, H. Song, J. Choi, J.S. Park, R. Ovalle-Robles, H.D. Yang, K.D. Kihm, R.H. Baughman, H.H. Lee, T.J. Kang, Y.H. Kim, High-efficiency electrochemical thermal energy harvester using carbon nanotube aerogel sheet electrodes, Nat. Commun. 7 (2016) 1–9, http://dx.doi.org/10.1038/ncomms10600.
[4] E. Laux, S. Uhl, N. Gauthier, L. Jeandupeux, H. Keppner, P. Pérez López, S. Pauline, E. Vanoli, R. Marti, Development of Thermoelectric generator based on Ionic Liquids for high temperature applications, Mater. Today Proc. 5 (2018) 10195–10202, http://dx.doi.org/10.1016/j.matpr.2017.12.265.
[5] M. Watanabe, M.L. Thomas, S. Zhang, K. Ueno, T. Yasuda, K. Dokko, Application of ionic liquids to energy storage and conversion materials and devices, Chem. Rev. 117 (2017) 7190–7239, http://dx.doi.org/10.1021/acs.chemrev.6b00504.
[6] D. Al-Masri, M. Dupont, R. Yunis, D.R. MacFarlane, J.M. Pringle, The electrochemistry and performance of cobalt-based redox couples for thermoelectrochemical cells, Electrochim. Acta 269 (2018) 714–723, http://dx.doi.org/10.1016/j.electacta.2018.03.032.
[7] T.J. Salez, B.T. Huang, M. Rietjens, M. Bonetti, C. Wiertel-Gasquet, M. Roger, C.L. Filomeno, E. Dubois, R. Perzynski, S. Nakamae, Can charged colloidal particles increase the thermoelectric energy conversion efficiency? Phys. Chem. Chem. Phys. 19 (2017) 9409–9416, http://dx.doi.org/10.1039/C7CP01023K.
[8] T. Salez, S. Nakamae, R. Perzynski, G. Mériguet, A. Cebers, M. Roger, Thermoelectricity and Thermodiffusion in Magnetic Nanofluids: Entropic Analysis, Entropy. 20 (2018) 405, http://dx.doi.org/10.3390/e20060405.
[9] B.T. Huang, M. Roger, M. Bonetti, T.J. Salez, C. Wiertel-Gasquet, E. Dubois, R. Cabreira Gomes, G. Demouchy, G. Mériguet, V. Peyre, M. Kouyaté, C.L. Filomeno, J. Depeyrot, F.A. Tourinho, R. Perzynski, S. Nakamae, Thermoelectricity and thermodiffusion in charged colloids, J. Chem. Phys. 143 (2015), http://dx.doi.org/10.1063/1.4927665.
[10] S. Hao, V.P. Dravid, M.G. Kanatzidis, C. Wolverton, Computational strategies for design and discovery of nanostructured thermoelectrics, Npj Comput. Mater. 5 (2019) 1–10, http://dx.doi.org/10.1038/s41524-019-0197-9.
[11] W. Zhao, Z. Liu, Z. Sun, Q. Zhang, P. Wei, X. Mu, H. Zhou, C. Li, S. Ma, D. He, P. Ji, W. Zhu, X. Nie, X. Su, X. Tang, B. Shen, X. Dong, J. Yang, Y. Liu, J. Shi, Superparamagnetic enhancement of thermoelectric performance, Nature 549 (2017) 247–251, http://dx.doi.org/10.1038/nature23667.
[12] K. Alberi, M.B. Nardelli, A. Zakutayev, L. Mitas, S. Curtarolo, A. Jain, M. Fornari, N. Marzari, I. Takeuchi, M.L. Green, M. Kanatzidis, M.F. Toney, S. Butenko, B. Meredig, S. Lany, U. Kattner, A. Davydov, E.S. Toberer, V. Stevanovic, A. Walsh, N.G. Park, A. Aspuru-Guzik, D.P. Tabor, J. Nelson, J. Murphy, A. Setlur, J. Gregoire, H. Li, R. Xiao, A. Ludwig, L.W. Martin, A.M. Rappe, S.H. Wei, J. Perkins, The 2019 materials by design roadmap, J. Phys. D Appl. Phys. 52 (2019), http://dx.doi.org/10.1088/1361-6463/aad926.
[13] K. Binder, Applications of the Monte-Carlo Method in Statistical Physics, Springer-Verlag, NY, 1987, http://dx.doi.org/10.1007/978-3-642-96788-7.
[14] M.R. Peterson, B.S. Shastry, Kelvin formula for thermopower, Phys. Rev. B 82 (2010) 195105(5), http://dx.doi.org/10.1103/PhysRevB.82.195105.
[15] A.A. Abrikosov, Fundamentals of the Theory of Metals, Elsevier B.V., North Holland, 1988.
[16] K.L. Pisane, S. Singh, M.S. Seehra, Unusual enhancement of effective magnetic anisotropy with decreasing particle size in maghemite nanoparticles, Appl. Phys. Lett. 110 (2017) 222409, http://dx.doi.org/10.1063/1.4984903.
[17] B.S. Shastry, Electrothermal transport coefficients at finite frequencies, Rep. Prog. Phys. 72 (2009), http://dx.doi.org/10.1088/0034-4885/72/1/016501.
[18] A.A. Varlamov, A.V. Kavokin, Prediction of thermomagnetic and thermoelectric properties for novel materials and systems, EPL (Europhysics Lett.) 103 (2013) 47005, http://dx.doi.org/10.1209/0295-5075/103/47005.
[19] E.C. Stoner, F.R.S. Wohlfarth, E.P. Wohlfarth, On a mechanism of magnetic hysteresis in heterogeneous alloys, Philos. Trans. Roy. Soc. London 240 (1948) 599, http://dx.doi.org/10.1098/rsta.1948.0007.
[20] G. Margaris, K.N. Trohidou, V. Iannotti, G. Ausanio, L. Lanotte, D. Fiorani, Magnetic behavior of dense nanoparticle assemblies: interplay of interparticle interactions and particle system morphology, Phys. Rev. B 86 (2012) 214425, http://dx.doi.org/10.1103/PhysRevB.86.214425.
[21] M. Vasilakaki, N. Ntallis, N. Yaacoub, G. Muscas, D. Peddis, K.N. Trohidou, Optimising the magnetic performance of Co ferrite nanoparticles via organic ligand capping, Nanoscale 10 (2018) 21244–21253, http://dx.doi.org/10.1039/c8nr04566f.
[22] L. Mohammed, H.G. Gomaa, D. Ragab, J. Zhu, Magnetic nanoparticles for environmental and biomedical applications: A review, Particuology 30 (2017) 1–14, http://dx.doi.org/10.1016/j.partic.2016.06.001.

[23] G. Muscas, N. Yaacoub, G. Concas, F. Sayed, R. Sayed Hassan, J.M. Greneche, C. Cannas, A. Musinu, V. Foglietti, S. Casciardi, C. Sangregorio, D. Peddis, Evolution of the magnetic structure with chemical composition in spinel iron oxide nanoparticles, Nanoscale 7 (2015) 13576–13585, http://dx.doi.org/10.1039/C5NR02723C.
[24] A.I. Figueroa, J. Bartolomé, L.M. García, F. Bartolomé, A. Arauzo, A. Millán, F. Palacio, Magnetic anisotropy of maghemite nanoparticles probed by RF transverse susceptibility, Phys. Procedia 75 (2015) 1050–1057, http://dx.doi.org/10.1016/j.phpro.2015.12.174.
[25] F. Gazeau, J.C. Bacri, F. Gendron, R. Perzynski, Y.L. Raikher, V.I. Stepanov, E. Dubois, Magnetic resonance of ferrite nanoparticles, J. Magn. Magn. Mater. 186 (1998) 175–187, http://dx.doi.org/10.1016/S0304-8853(99)00156-0202.
[26] G.C. Papaefthymiou, E. Devlin, A. Simopoulos, D.K. Yi, S.N. Riduan, S.S. Lee, J.Y. Ying, Interparticle interactions in magnetic core/shell nanoarchitectures, Phys. Rev. B 80 (2009) 24406, http://dx.doi.org/10.1103/PhysRevB.80.024406.
[27] A.P. Safronov, I.V. Beketov, S.V. Komogortsev, G.V. Kurlyandskaya, A.I. Medvedev, D.V. Leiman, A. Larrañaga, S.M. Bhagat, Spherical magnetic nanoparticles fabricated by laser target evaporation, AIP Adv. 3 (2013), http://dx.doi.org/10.1063/1.4808368.
[28] D. Fiorani, A.M. Testa, F. Lucari, F.D. Orazio, H. Romero, Magnetic properties of maghemite nanoparticle systems: surface anisotropy and interparticle interaction effects, Phys. B 320 (2002) 122–126, http://dx.doi.org/10.1016/S0921-4526(02)00659-2.
[29] W. Baaziz, B.P. Pichon, S. Fleutot, Y. Liu, C. Lefevre, J. Greneche, M. Toumi, T. Mhiri, S. Begin-colin, Magnetic Iron oxide nanoparticles: reproducible tuning of the size and nanosized-dependent composition, defects, and spin canting, J. Phys. Chem. C 118 (2014) 3795–3810, http://dx.doi.org/10.1021/jp411481p.
[30] P. Priyananda, H. Sabouri, N. Jain, B.S. Hawkett, Steric stabilization of γ-Fe2O3Superparamagnetic nanoparticles in a hydrophobic ionic liquid and the magnetorheological behavior of the ferrofluid, Langmuir 34 (2018) 3068–3075, http://dx.doi.org/10.1021/acs.langmuir.7b04291.
[31] P.V. Hendriksen, S. Linderoth, P.A. Lindgård, Finite-size modifications of the magnetic properties of clusters, Phys. Rev. B 48 (1993) 7259–7273, http://dx.doi.org/10.1103/PhysRevB.48.7259.
[32] S. Yoon, K.M. Krishnan, Temperature dependence of magnetic anisotropy constant in manganese ferrite nanoparticles at low temperature, J. Appl. Phys. 109 (2011) 3–5, http://dx.doi.org/10.1063/1.3563068.
[33] B.K. Chatterjee, C.K. Ghosh, K.K. Chattopadhyay, Temperature dependence of magnetization and anisotropy in uniaxial $NiFe_2O_4$ nanomagnets: deviation from the Callen-Callen power law, J. Appl. Phys. 116 (2014) 153904, http://dx.doi.org/10.1063/1.4898089.
[34] J. Wang, F. Zhao, W. Wu, G.M. Zhao, Unusual temperature dependence of the magnetic anisotropy constant in barium ferrite $BaFe_{12}O_{19}$, J. Appl. Phys. 110 (2011) 10–13, http://dx.doi.org/10.1063/1.3657851.
[35] S. Bedanta, W. Kleemann, Supermagnetism, J. Phys. D Appl. Phys. 42 (2009), http://dx.doi.org/10.1088/0022-3727/42/1/013001.
[36] N. Ntallis, M. Vasilakaki, D. Peddis, K.N. Trohidou, Effect of organic coating on the charge distribution of $CoFe_2O_4$ nanoparticles, J. Alloys. Compd. 796 (2019) 9–12, http://dx.doi.org/10.1016/j.jallcom.2019.05.042.
[37] D. Peddis, C. Cannas, A. Musinu, A. Ardu, F. Orrù, D. Fiorani, S. Laureti, D. Rinaldi, G. Muscas, G. Concas, G. Piccaluga, Beyond the effect of particle size: influence of $CoFe_2O_4$ nanoparticle arrangements on magnetic properties, Chem. Mater. 25 (2013) 2005–2013, http://dx.doi.org/10.1021/cm303352r.
[38] K. Maaz, M. Usman, S. Karim, A. Mumtaz, S.K. Hasanain, M.F. Bertino, Magnetic response of core-shell cobalt ferrite nanoparticles at low temperature Tuning of magnetic properties in cobalt ferrite nanocrystals magnetic response of core-shell cobalt ferrite nanoparticles at low temperature, J. Appl. Phys. 105 (2009) 113917–252405, http://dx.doi.org/10.1063/1.3139293.
[39] S. Yoon, Temperature dependence of magnetic anisotropy constant in cobalt ferrite nanoparticles, J. Magn. Magn. Mater. 324 (2012) 2620–2624, http://dx.doi.org/10.1016/j.jmmm.2012.03.019.
[40] Y. Zhang, Y. Liu, C. Fei, Z. Yang, Z. Lu, R. Xiong, D. Yin, J. Shi, The temperature dependence of magnetic properties for cobalt ferrite nanoparticles by the hydrothermal method, J. Appl. Phys. 108 (2010) 1–7, http://dx.doi.org/10.1063/1.3499289.
[41] M. Grigorova, H.J. Blythe, V. Blaskov, V. Rusanov, V. Petkov, V. Masheva, D. Nihtianova, L.M. Martinez, J.S. Muñoz, M. Mikhov, Magnetic properties and Mössbauer spectra of nanosized $CoFe_2O_4$ powders, J. Magn. Magn. Mater. 183 (1998) 163–172, http://dx.doi.org/10.1016/S0304-8853(97)01031-7.
[42] T.E. Torres, A.G. Roca, M.P. Morales, A. Ibarra, C. Marquina, M.R. Ibarra, G.F. Goya, Magnetic properties and energy absorption of $CoFe_2O_4$ nanoparticles for magnetic hyperthermia, J. Phys. Conf. Ser. 200 (2010) 72101, http://dx.doi.org/10.1088/1742-6596/200/7/072101.